

Magnetostriction in transversely isotropic hexagonal crystalsGiancarlo Consolo^{1,*}, Salvatore Federico², and Giovanna Valenti³¹*Department of Mathematical, Computer, Physical and Earth Sciences, University of Messina, Viale F. Stagno D'Alcontres 31, 98166 Vill. S. Agata, Messina, Italy*²*Department of Mechanical and Manufacturing Engineering, The University of Calgary, Calgary, Alberta, Canada T2N 1N4*³*Department of Engineering, University of Messina, Contrada di Dio, 98166 Vill. S. Agata, Messina, Italy*

(Received 19 July 2019; revised manuscript received 13 December 2019; published 6 January 2020)

The simultaneous occurrence of direct and inverse magnetostriction in transversely isotropic hexagonal crystal is theoretically investigated. Particular emphasis is here given to the need of identifying the fourth-order magnetostriction tensor, as it represents the most primitive object from which all related physical quantities of interest in micromagnetism are deduced. For hexagonal crystals, the magnetostriction tensor is expressed in terms of six independent magnetostrictive coefficients whose values are, so far, unknown. Indeed, the existing literature provides just four independent constraints that are extracted from the expression of the differential scalar strain in a given direction. In this work, the two extra conditions required to solve this identification problem are obtained by deducing the explicit functional dependence of the main features characterizing the motion of a magnetic domain wall along the major axis of a thin magnetostrictive nanostrip placed on the top of a thick piezoelectric actuator. The results of our analysis reveal that such two conditions may be associated to the effective anisotropy coefficient and the domain-wall width. To validate our proposal, a comparison with some recent experimental results is also successfully addressed.

DOI: [10.1103/PhysRevB.101.014405](https://doi.org/10.1103/PhysRevB.101.014405)**I. INTRODUCTION**

Multifunctional materials for next-generation devices exploit the control of the magnetic state via electric fields and vice versa. These materials are attracting a great deal of attention for their potential applications in several fields, ranging from spintronic (memory and logic) devices to solid-state transformers, from magnetic/electric field sensors to electromagnetic actuators [1–3]. The success of these devices relies on the possibility of achieving a relatively large magneto-electric coupling by encapsulating (gluing or depositing), for instance, a magnetic nanodevice into a piezoelectric environment [4–9]. In such artificial composite structures, generally termed *magnetolectric multiferroics*, magnetic and electric order parameters are simultaneously present and coupled with each other. Indeed, when a piezoelectric actuator deforms upon the application of an electric field, it imposes displacements, and thus strains, on the ferromagnetic strip through the common interface. Owing to magnetoelastic interactions, such strains induce changes of the overall magnetic anisotropy field that are, in turn, converted into modifications of the magnetic configuration (via the inverse magnetostrictive effect) [2,4,5,8,9]. At the same time, the ferromagnetic layer is also subjected to the stress-free strain caused by magnetostriction so that both direct (Joule) and inverse (Villari) magnetostrictive effects take place simultaneously [10–12].

In this context, a key role is played by the crystal symmetry of the magnetic material since, as known, it affects anisotropy, and magnetoelastic and magnetostrictive energies

[10–12]. The need of obtaining sizable magnetoelectric coupling that has, at the same time, good chemical and mechanical properties, is indeed currently pushing the research toward the study of novel materials. Among the most interesting and investigated ones, we recall $\text{Tb}_{1-x}\text{Dy}_x\text{Fe}_2$ (terfenol-D), CoFe_2O_4 , NiFe_2O_4 , Ga-Fe (galfenol) alloys, Co-Pt, Ni-Mn-Ga, $\text{BaFe}_{12}\text{O}_{19}$ and other ferrites and manganites, whose crystal structure belongs, in most cases, to the cubic or hexagonal classes. In this work, we limit our analysis to the subclass of hexagonal systems that exhibit transverse isotropy and that are rather poorly theoretically studied despite their huge applications.

To properly characterize magnetostrictive and magnetoelastic effects taking place in such materials, the knowledge of the fourth-order magnetostriction tensor is required. Unfortunately, the recent literature has somehow overlooked its relevance despite it constitutes the most primitive object which allows to deduce all the related quantities, e.g., the second-order magnetostrictive strain tensor, the scalar magnetostrictive strain in a given direction, and the magnetoelastic field. This latter represents an additive contribution to the effective magnetic field that has to be taken into account in a micromagnetic model when magnetic and mechanical effects take place simultaneously.

For hexagonal transversely isotropic crystals, the fourth-order magnetostriction tensor is expressed through *six* independent coefficients which are, so far, unknown. This indeterminacy prevents the possibility to carry out an analytical investigation in the framework of micromagnetism and, indeed, theoretical works reduce the analysis to the simplest case of an isotropic medium [4,6,13–15] or tackle the study of cubic symmetries, where the magnetostriction tensor is

*Corresponding author: gconsolo@unime.it

fully known [16–22]. In our view, the above gap is generated by the fact that a former relevant paper [23] focused on the characterization of the scalar magnetostrictive strain in an arbitrary direction, a quantity that involves just *four* independent conditions on magnetostrictive coefficients. Therefore, two additional independent constraints are required to achieve the full identification of the magnetostriction tensor and, thus, to directly quantify the magnetoelastic field. This work is an attempt to fill this gap.

The paper is organized as outlined below. In Sec. II, we discuss the theoretical background on magnetostriction for hexagonal crystals. Preliminarily, we recall the concepts of second- and fourth-order magnetostriction tensors and show how to deduce the explicit expressions of magnetoelastic and magnetocrystalline anisotropy fields. At the end of the section, we focus the attention on some key remarks about the still-open question on the indeterminacy of the six components of fourth-order magnetostriction tensor. In Sec. III, we address analytical investigations on the domain-wall motion in a bilayer piezoelectric-magnetostrictive device under the simultaneous effects arising from magnetic fields, electric currents, magnetostriction, and applied strains. This study is finalized at extracting and inspecting the magnetostrictive dependence of the main features here involved. As a result of this analysis, we deduce the two extra conditions required to solve the aforementioned identification problem, as reported in Sec. III A. In Section. IV, we carry out some numerical investigations to estimate quantitatively the values of all the six magnetostrictive coefficients and validate our proposal. To this purpose, we take into account literature data on cobalt and cobalt-platinum alloys. Concluding remarks are given in Sec. V.

II. THEORETICAL BACKGROUND ON MAGNETOSTRICTION

For a ferromagnetic magnetostrictive material, the infinitesimal strain tensor ϵ , which is *compatible* since it is defined as the symmetric part of the displacement gradient $\nabla \mathbf{u}$, can be additively decomposed into

$$\epsilon = \epsilon^e + \epsilon^m, \quad (1)$$

where the two *incompatible* strain tensors ϵ^e and ϵ^m are the elastic and magnetostrictive strains, respectively [16,21,24]. For a linear elastic material, the elastic energy density is quadratic and expressed as

$$E^e = \frac{1}{2} \epsilon^e : \mathbb{C} : \epsilon^e = \frac{1}{2} \epsilon_{ij}^e C_{ijkl} \epsilon_{kl}^e, \quad (2)$$

where \mathbb{C} is the fourth-order elasticity (or stiffness) tensor and “:” denotes the double contraction. The elasticity tensor \mathbb{C} enjoys minor symmetry on both pairs of indices (i.e., $C_{ijkl} = C_{jikl} = C_{ijlk} = C_{jilk}$) as well as major symmetry (i.e., $C_{ijkl} = C_{klij}$) (see, e.g., [25–27]). By differentiating the elastic energy $E^e = \hat{E}^e(\epsilon^e)$ with respect to ϵ^e and exploiting the major symmetry of \mathbb{C} , we obtain the Cauchy stress as

$$\sigma = \frac{\partial \hat{E}^e}{\partial \epsilon^e}(\epsilon^e) = \mathbb{C} : \epsilon^e, \quad \sigma_{ij} = \frac{\partial \hat{E}^e}{\partial \epsilon_{ij}^e}(\epsilon^e) = C_{ijkl} \epsilon_{kl}^e. \quad (3)$$

In the remainder of this work, for the components C_{ijkl} of the elasticity tensor \mathbb{C} , we adopt Voigt’s compact notation,

through which fourth-order tensors with minor symmetries on both pairs of indices can be represented by a 6×6 matrix.

The hexagonal crystal classes $\bar{6}m2$, $6mm$, 622 , and $6/mmm$ here investigated exhibit transverse isotropy, i.e., invariance under rotations about a given direction, called direction of symmetry, which we choose to be $\mathbf{e}_z \equiv \mathbf{e}_3$. For this class, the elasticity tensor \mathbb{C} can be expressed in terms of five independent elastic constants c_{11} , c_{12} , c_{13} , c_{33} , and c_{44} , such that

$$[\mathbb{C}] = \begin{bmatrix} c_{11} & c_{12} & c_{13} & & & \\ c_{12} & c_{11} & c_{13} & & & \\ c_{13} & c_{13} & c_{33} & & & \\ & & & c_{44} & 0 & 0 \\ & & & 0 & c_{44} & 0 \\ & & & 0 & 0 & \frac{c_{11}-c_{12}}{2} \end{bmatrix}. \quad (4)$$

Using the decomposition (1) and the major symmetry of the elasticity tensor \mathbb{C} , the elastic energy density (2) can be split into three parts:

$$E^e = \frac{1}{2} \epsilon : \mathbb{C} : \epsilon - \epsilon : \mathbb{C} : \epsilon^m + \frac{1}{2} \epsilon^m : \mathbb{C} : \epsilon^m. \quad (5)$$

The first term

$$E = \frac{1}{2} \epsilon : \mathbb{C} : \epsilon \quad (6)$$

is the *total strain energy density* and is the only contribution which is implicitly dependent on magnetization, whereas the other two terms

$$E^{\text{me}} = -\epsilon : \mathbb{C} : \epsilon^m, \quad (7a)$$

$$E^{\text{ms}} = \frac{1}{2} \epsilon^m : \mathbb{C} : \epsilon^m \quad (7b)$$

represent the *magnetoelastic energy density* and the *magnetostrictive energy density*, respectively, and are both explicitly dependent on the magnetization configuration \mathbf{m} via the magnetostrictive strain ϵ^m [16,17,20,28].

The presence of magnetization-dependent terms into the elastic energy E^e gives rise to a magnetic field

$$\mathbf{h}^{\text{me}} = -\frac{1}{\mu_0 M_S^2} \frac{\delta \hat{E}^e}{\delta \mathbf{m}}(\mathbf{m}), \quad (8)$$

commonly referred to as the *magnetoelastic field*. In Eq. (8), μ_0 is the magnetic permeability of vacuum, M_S is the magnitude of the magnetization at saturation, and the differential operator $\delta/\delta \mathbf{m}$ represents the variational derivative defined as

$$\frac{\delta}{\delta m_i} = \frac{\partial}{\partial m_i} - \frac{\partial}{\partial x_j} \frac{\partial}{\partial m_{i,j}}, \quad (9)$$

where $m_{i,j} \equiv \partial m_i / \partial x_j$ are the components of the gradient $\nabla \mathbf{m}$ in the usual index notation. Therefore, according to (5), \mathbf{h}^{me} can be recast as

$$\begin{aligned} \mathbf{h}^{\text{me}} &= -\frac{1}{\mu_0 M_S^2} \frac{\partial (\hat{E}^{\text{me}} + \hat{E}^{\text{ms}})}{\partial \mathbf{m}}(\mathbf{m}) \\ &= \frac{1}{\mu_0 M_S^2} (\epsilon - \epsilon^m) : \mathbb{C} : \frac{\partial \epsilon^m}{\partial \mathbf{m}} \end{aligned} \quad (10)$$

since the magnetostrictive strain ϵ^m is independent of $\nabla \mathbf{m}$ [16,20,21].

Equation (10) reveals that the symmetry of the crystal affects the magnetoelastic field via the elasticity tensor \mathbb{C} and the magnetostriction tensor \mathbb{Z} through the magnetostrictive strain tensor $\epsilon^m = \mathbb{Z} : \mathbf{m} \otimes \mathbf{m}$. The expression of the elasticity tensor \mathbb{C} is well known in the literature for all crystal classes (see, e.g., [29]). On the other hand, the second-order magnetostrictive strain tensor ϵ^m is deduced through the knowledge of a more primitive object, the fourth-order magnetostriction tensor \mathbb{Z} , whose comprehensive characterization for all crystal classes has been done in our recent work [30]. We recall that the magnetostriction tensor \mathbb{Z} always enjoys minor symmetry

on both pairs of indices, i.e.,

$$Z_{ijkl} = Z_{jikl} = Z_{ijlk} = Z_{jilk}, \quad (11)$$

but it does not possess, in general, major symmetry: $Z_{ijkl} \neq Z_{klij}$.

For a transversely isotropic material, the fourth-order magnetostriction tensor \mathbb{Z} is defined through six independent magnetostriction coefficients Z_{1111} , Z_{1122} , Z_{1133} , Z_{3311} , Z_{3333} , and Z_{2323} , and its representing 6×6 matrix reads as [29,30]

$$[\mathbb{Z}] = \begin{bmatrix} Z_{1111} & Z_{1122} & Z_{1133} & & & \\ Z_{1122} & Z_{1111} & Z_{1133} & & & \\ Z_{3311} & Z_{3311} & Z_{3333} & & & \\ & [0] & & Z_{2323} & 0 & 0 \\ & & & 0 & Z_{2323} & 0 \\ & & & 0 & 0 & \frac{1}{2}(Z_{1111} - Z_{1122}) \end{bmatrix}. \quad (12)$$

Let us here stress that expression (12) refers to the general, *nonisochoric*, case, which is the one taken into account in the literature [23,31–34]. Once the tensor \mathbb{Z} is known, we can compute both [14,21,23,24,30–32] the second-order magnetostrictive strain tensor ϵ^m as

$$\epsilon^m = \mathbb{Z} : (\mathbf{m} \otimes \mathbf{m}), \quad \epsilon_{ij}^m = Z_{ijkl} m_k m_l \quad (13)$$

and the (measurable) scalar magnetostriction λ_n along a given direction \mathbf{n} , i.e.,

$$\lambda_n = (\mathbf{n} \otimes \mathbf{n}) : \mathbb{Z} : (\mathbf{m} \otimes \mathbf{m}) = n_i n_j Z_{ijkl} m_k m_l. \quad (14)$$

By virtue of (12), the magnetostriction strain tensor ϵ^m has matrix representation [30]

$$[\epsilon^m] = \begin{bmatrix} Z_{1111} m_x^2 + Z_{1122} m_y^2 + Z_{1133} m_z^2 & (Z_{1111} - Z_{1122}) m_x m_y & 2Z_{2323} m_x m_z \\ (Z_{1111} - Z_{1122}) m_x m_y & Z_{1122} m_x^2 + Z_{1111} m_y^2 + Z_{1133} m_z^2 & 2Z_{2323} m_y m_z \\ 2Z_{2323} m_x m_z & 2Z_{2323} m_y m_z & Z_{3311} m_x^2 + Z_{3311} m_y^2 + Z_{3333} m_z^2 \end{bmatrix}. \quad (15)$$

However, some classical papers on hexagonal crystals [31,32], rather than using the above expression for the magnetostrictive strain tensor, report the *differential* value measured with respect to the configuration in which the material is magnetized along its *easy* direction \mathbf{a}_{easy} . For instance, in MnAs- and Co-based materials, the easy direction of magnetization lies in plane and normal to plane, respectively. Restricting our attention to Co-based materials, we set $\mathbf{a}_{\text{easy}} \equiv \mathbf{e}_z$ and obtain

$$[\Delta \epsilon^m] = [\epsilon^m] - [\epsilon^m]_{m_z=1} = \begin{bmatrix} (Z_{1111} - Z_{1133}) m_x^2 + (Z_{1122} - Z_{1133}) m_y^2 & (Z_{1111} - Z_{1122}) m_x m_y & 2Z_{2323} m_x m_z \\ (Z_{1111} - Z_{1122}) m_x m_y & (Z_{1122} - Z_{1133}) m_x^2 + (Z_{1111} - Z_{1133}) m_y^2 & 2Z_{2323} m_y m_z \\ 2Z_{2323} m_x m_z & 2Z_{2323} m_y m_z & (Z_{3311} - Z_{3333})(1 - m_z^2) \end{bmatrix}, \quad (16)$$

from which we deduce the expression for the differential scalar strain [23]:

$$\begin{aligned} \Delta \lambda_n &= \Delta \epsilon^m : \mathbf{n} \otimes \mathbf{n} = (Z_{1111} - Z_{1133})[(m_x n_x + m_y n_y)^2 - m_z n_z (m_x n_x + m_y n_y)] \\ &\quad + (Z_{1122} - Z_{1133})[(1 - m_z^2)(1 - n_z^2) - (m_x n_x + m_y n_y)^2] \\ &\quad + (Z_{3311} - Z_{3333})[n_z^2(1 - m_z^2) - m_z n_z (m_x n_x + m_y n_y)] \\ &\quad + (Z_{1111} - Z_{1133} + Z_{3311} - Z_{3333} + 4Z_{2323})m_z n_z (m_x n_x + m_y n_y). \end{aligned} \quad (17)$$

Moreover, to keep the notation on magnetostrictive strains as close as possible to the one used in the consolidated literature, we recast (15) as in Ref. [32]:

$$[\epsilon^m] = \begin{bmatrix} (\lambda_A - \lambda_B) m_x^2 - \lambda_B m_z^2 + \lambda_B + \lambda_{13} & (\lambda_A - \lambda_B) m_x m_y & \lambda_E m_x m_z \\ (\lambda_A - \lambda_B) m_x m_y & (\lambda_A - \lambda_B) m_y^2 - \lambda_B m_z^2 + \lambda_B + \lambda_{13} & \lambda_E m_y m_z \\ \lambda_E m_x m_z & \lambda_E m_y m_z & \lambda_C (1 - m_z^2) + \lambda_{33} \end{bmatrix}, \quad (18)$$

where the coefficients λ_A , λ_B , λ_C , λ_E , λ_{13} , and λ_{33} are defined by [23,31,32]

$$\lambda_A = Z_{1111} - Z_{1133}, \quad (19a)$$

$$\lambda_B = Z_{1122} - Z_{1133}, \quad (19b)$$

$$\lambda_C = Z_{3311} - Z_{3333}, \quad (19c)$$

$$\lambda_E = 2 Z_{2323}, \quad (19d)$$

$$\lambda_{13} = Z_{1133}, \quad (19e)$$

$$\lambda_{33} = Z_{3333}. \quad (19f)$$

Therefore, the total elastic energy can be expressed as

$$E = \frac{1}{2}c_{11}(\epsilon_{xx}^2 + \epsilon_{yy}^2) + c_{12}\epsilon_{xx}\epsilon_{yy} + c_{13}\epsilon_{zz}(\epsilon_{xx} + \epsilon_{yy}) + \frac{1}{2}c_{33}\epsilon_{zz}^2 + 2c_{44}(\epsilon_{xz}^2 + \epsilon_{yz}^2) + (c_{11} - c_{12})\epsilon_{xy}^2, \quad (20)$$

whereas the differential magnetoelastic and magnetostrictive energies are given by [35–38]

$$\begin{aligned} \Delta E^{\text{me}} = & (\lambda_A - \lambda_B)(c_{12} - c_{11})(\epsilon_{xx}m_x^2 + \epsilon_{yy}m_y^2 + 2\epsilon_{xy}m_xm_y) - [(\lambda_A + \lambda_B)c_{13} + \lambda_Cc_{33}](1 - m_z^2)\epsilon_{zz} \\ & - [\lambda_Ac_{12} + \lambda_Bc_{11} + \lambda_Cc_{13}](1 - m_z^2)(\epsilon_{xx} + \epsilon_{yy}) - 4c_{44}\lambda_E(\epsilon_{xz}m_x + \epsilon_{yz}m_y)m_z, \end{aligned} \quad (21a)$$

$$\begin{aligned} \Delta E^{\text{ms}} = & (c_{11} + c_{12})\lambda_B\{[\lambda_Bm_z^2 - (\lambda_A - \lambda_B)(m_x^2 + m_y^2)]m_z^2 + \lambda_B + 2\lambda_{13}\} \\ & + \frac{1}{2}c_{11}(\lambda_A - \lambda_B)^2(m_x^2 + m_y^2)^2 + 2c_{13}[\lambda_C(\lambda_B + \lambda_{13})(1 - m_z^2) + \lambda_B\lambda_{33}] \\ & + [(\lambda_A - \lambda_B)(m_x^2 + m_y^2) - 2\lambda_Bm_z^2]\{(c_{11} + c_{12})(\lambda_B + \lambda_{13}) + c_{13}[\lambda_C(1 - m_z^2) + \lambda_{33}]\} \\ & + \frac{1}{2}c_{33}\lambda_C(1 - m_z^2)[\lambda_C(1 - m_z^2) + 2\lambda_{33}] + 2c_{44}\lambda_E^2m_z^2(m_x^2 + m_y^2). \end{aligned} \quad (21b)$$

From (21a) and (21b), we deduce the components of the magnetoelastic field (10) as

$$\begin{aligned} h_x^{\text{me}} = & \frac{2}{\mu_0M_S^2}((\lambda_A - \lambda_B)m_x\{c_{11}[\epsilon_{xx} - (\lambda_A - \lambda_B)m_x^2 + \lambda_Bm_z^2 - (\lambda_B + \lambda_{13})] \\ & + c_{12}[\epsilon_{yy} - (\lambda_A - \lambda_B)m_y^2 + \lambda_Bm_z^2 - (\lambda_B + \lambda_{13})] + c_{13}[\epsilon_{zz} + \lambda_Cm_z^2 - (\lambda_C + \lambda_{33})]\} \\ & + 2c_{44}(\epsilon_{xz} - \lambda_Em_xm_z)\lambda_Em_z + (c_{11} - c_{12})[\epsilon_{xy} - (\lambda_A - \lambda_B)m_xm_y](\lambda_A - \lambda_B)m_y), \end{aligned} \quad (22a)$$

$$\begin{aligned} h_y^{\text{me}} = & \frac{2}{\mu_0M_S^2}((\lambda_A - \lambda_B)m_y\{c_{12}[\epsilon_{xx} - (\lambda_A - \lambda_B)m_x^2 + \lambda_Bm_z^2 - (\lambda_B + \lambda_{13})] \\ & + c_{11}[\epsilon_{yy} - (\lambda_A - \lambda_B)m_y^2 + \lambda_Bm_z^2 - (\lambda_B + \lambda_{13})] + c_{13}[\epsilon_{zz} + \lambda_Cm_z^2 - (\lambda_C + \lambda_{33})]\} \\ & + 2c_{44}(\epsilon_{yz} - \lambda_Em_y m_z)\lambda_Em_z + (c_{11} - c_{12})(\epsilon_{xy} - (\lambda_A - \lambda_B)m_xm_y)(\lambda_A - \lambda_B)m_x), \end{aligned} \quad (22b)$$

$$\begin{aligned} h_z^{\text{me}} = & \frac{2}{\mu_0M_S^2}(-\lambda_Bm_z\{(c_{11} + c_{12})[\epsilon_{xx} + \epsilon_{yy} - (\lambda_A - \lambda_B)(m_x^2 + m_y^2) + 2\lambda_Bm_z^2 - 2(\lambda_B + \lambda_{13})] \\ & + 2c_{13}(\epsilon_{zz} + \lambda_Cm_z^2 - \lambda_C - \lambda_{33})\} - \lambda_Cm_z\{c_{13}[\epsilon_{xx} + \epsilon_{yy} - (\lambda_A - \lambda_B)(m_x^2 + m_y^2) + 2\lambda_Bm_z^2 - 2(\lambda_B + \lambda_{13})] \\ & + c_{33}(\epsilon_{zz} + \lambda_Cm_z^2 - \lambda_C - \lambda_{33})\} + 2c_{44}\lambda_E[(\epsilon_{yz} - \lambda_Em_y m_z)m_y + (\epsilon_{xz} - \lambda_Em_x m_z)m_x]). \end{aligned} \quad (22c)$$

Let us emphasize that, in the context of micromagnetism, the crystal symmetry of the ferromagnetic material also affects the magnetocrystalline anisotropy field which can be deduced from the corresponding anisotropy energy $E^{\text{ani}} = \hat{E}^{\text{ani}}(\mathbf{m})$ as

$$\mathbf{h}^{\text{me}} = -\frac{1}{\mu_0M_S^2} \frac{\partial \hat{E}^{\text{ani}}}{\partial \mathbf{m}}(\mathbf{m}), \quad (23)$$

where the functional dependence of E^{ani} on the magnetization \mathbf{m} is indeed specified by the crystal symmetry.

For hexagonal crystals with easy-axis direction along \mathbf{e}_z , the magnetocrystalline anisotropy energy density reads

as

$$E^{\text{ani}} = -K_A(\mathbf{m} \cdot \mathbf{e}_z)^2, \quad (24)$$

where K_A is the uniaxial anisotropy coefficient so that

$$\mathbf{h}^{\text{ani}} = \frac{2K_A}{\mu_0M_S^2}(\mathbf{m} \cdot \mathbf{e}_z)\mathbf{e}_z. \quad (25)$$

Remark 1. The magnetostriction tensor (12) refers to the general case of a transversely isotropic material for which the magnetostrictive strain is *nonisochoric*. To account for a material undergoing *isochoric* magnetostrictive strains, it suffices to consider the constraints $Z_{1133} = -\frac{1}{2}Z_{3333}$ and $Z_{3311} = -(Z_{1111} + Z_{1122})$, as reported in our previous work [30]. As a

consequence of these constraints, the number of independent magnetostriction constants (19) reduces to four, i.e.,

$$\lambda_A = Z_{1111} + \frac{1}{2}Z_{3333}, \quad (26a)$$

$$\lambda_B = Z_{1122} + \frac{1}{2}Z_{3333}, \quad (26b)$$

$$\lambda_E = 2Z_{2323}, \quad (26c)$$

$$\lambda_{33} = Z_{3333}, \quad (26d)$$

while the other two constants are linearly dependent on (26) through

$$\lambda_C = -\lambda_A - \lambda_B, \quad (27a)$$

$$\lambda_{13} = -\frac{1}{2}\lambda_{33}. \quad (27b)$$

Remark 2. In some works (e.g., [32]), the magnetostrictive strain tensor ϵ^m given in (18) is described through four independent constants (λ_A , λ_B , λ_C , and λ_E), instead of the six required by the transversely isotropic hexagonal crystal class. This should *not* lead to the erroneous conclusion that an isochoric magnetostrictive deformation is there assumed, as one can argue from the lack of the terms λ_{13} and λ_{33} (see Remark 1). This apparent contradiction could be explained by arguing that, in those works, the authors are representing the differential strain $\Delta\epsilon^m$ instead of ϵ^m .

Remark 3. In order to compare our results with those by Mason [23], we have to keep in mind that he defined the second-order magnetostriction tensor as $\epsilon_{ij}^m = M_{ijkl} m_i m_j$. Thus, comparing with our Eq. (13), we note that Mason's tensor \mathbb{M} is the *transpose* of our \mathbb{Z} , i.e., $M_{ijkl} = Z_{klij}$. This being said, we noticed a missing factor $\frac{1}{2}$ in the expression of $M_{1212} \equiv Z_{1212}$ in Mason's Eq. (2)₄, which we understand is a misprint, as it has no repercussions in his subsequent calculations. More importantly, in the expression of the differential scalar strain $\Delta\lambda_n$, Mason erroneously reports a prefactor 2 for Z_{2323} , in place of the correct prefactor 4, as can be noticed by comparing his Eq. (14) with our Eq. (17). This mistake may not have relevant consequences as far as the analysis is restricted to the use of *differential* quantities that, as mentioned earlier, require the knowledge of four magnetostriction constants only, one of which incorporates the term $4Z_{2323}$. On the contrary, if the investigation involves *nondifferential* quantities, as it is the case for the magnetoelastic field (22), a still unsolved question is how to properly identify *all* the six magnetostriction coefficients appearing therein. Indeed, since the number of linearly independent measurement setups that can be arranged to compute the differential scalar strain in a given direction is restricted to four, two additional conditions are needed to close the system. To the best of our knowledge, this identification problem has never been addressed before and, indeed, the values of the magnetostriction constants for transversely isotropic systems (Z_{1111} , Z_{1122} , Z_{1133} , Z_{3311} , Z_{3333} , and Z_{2323}) are not available in the literature. We shall address this point in the next section.

III. STRAIN-MEDIATED DOMAIN-WALL MOTION

The solution of the identification problem presented at the end of Sec. II requires two additional independent constraints on the magnetostrictive coefficients to be found. To achieve this goal, we need a setup that meets the following

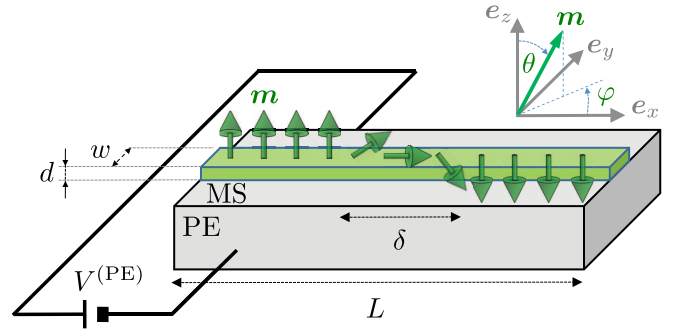


FIG. 1. Schematics of the bilayer piezoelectric-magnetostrictive (PE-MS) heterostructure, together with the reference frame.

requirements and is also of interest for the scientific community: (i) both the direct and the inverse magnetostriction phenomena take place simultaneously; (ii) its mathematical description allows to deduce, explicitly, the analytical functional dependence of the most relevant (and measurable) quantities on the magnetostriction coefficients.

A geometry that exhibits all the above features consists of a thin magnetostrictive (MS) nanostrip deposited or glued on the top surface of a thick piezoelectric (PE) actuator, as depicted in Fig. 1. This system is typically used in the literature to explore and emphasize magnetoelastic effects [4–9]. In such a device, it is assumed that a domain wall (DW) is initially nucleated at the center of the MS layer characterized by length L , width w , and thickness d along e_x , e_y , e_z axes, respectively, with $L \gg w > d$. The position of the DW along the major axis e_x is controlled by an external bias magnetic field \mathbf{h}^{ext} and/or an electric current density $\mathbf{J} = J\mathbf{e}_x$, which are both constant in time and uniform in space. On the other hand, the PE layer undergoes deformations upon the application of an electric voltage $V^{(\text{PE})}$ imposed between two lateral electrodes. These electrodes generate an electric field directed along the axis e_y that, depending on the sign of $V^{(\text{PE})}$, induces an elongation (contraction) of the bar width accompanied by a contraction (elongation) in the two orthogonal directions. Owing to the large thickness of the PE layer, the out-of-plane normal strain is generally negligible whereas all the shear strains are disregarded everywhere in the PE layer [4].

The magnetization dynamics occurring in the MS layer is ruled by the extended Landau-Lifshitz-Gilbert (ELLG) equation which, in the presence of spin-torque effects, reads as [39–49]

$$\dot{\mathbf{m}} = \gamma \mathbf{h}^{\text{eff}} \wedge \mathbf{m} + \mathbf{t}^{\text{stt}} + \mathbf{t}^{\text{d}}, \quad (28)$$

where, under the assumption of one-dimensional motion in direction x [42,43,47,48,50–59], the normalized magnetization vector takes the form $\mathbf{m}(x, t) = \mathbf{M}(x, t)/M_S$. In Eq. (28), the superposed dot denotes partial time derivative, $\gamma = M_S \mu_0 \gamma_e$ is a constant expressed in terms of the magnetic permeability of the vacuum μ_0 and of the gyromagnetic ratio $\gamma_e = g e / m_e$, being g the Landè factor, e the electron charge, and m_e the electron mass. The three terms appearing on the right-hand side of Eq. (28) describe the undamped precessional torque induced by the effective magnetic field \mathbf{h}^{eff} , the current-induced spin-transfer torque and the intrinsic damping torque, respectively. In detail, the effective magnetic field \mathbf{h}^{eff}

accounts for external, exchange, demagnetizing, magnetoelastic, and magnetocrystalline anisotropy contributions, i.e.,

$$\mathbf{h}^{\text{eff}} = \mathbf{h}^{\text{ext}} + \mathbf{h}^{\text{exc}} + \mathbf{h}^{\text{dmg}} + \mathbf{h}^{\text{me}} + \mathbf{h}^{\text{ani}}, \quad (29)$$

being

$$\mathbf{h}^{\text{ext}} = h_x \mathbf{e}_x + h_y \mathbf{e}_y + h_z \mathbf{e}_z, \quad (30a)$$

$$\mathbf{h}^{\text{exc}} = A \frac{\partial^2 \mathbf{m}}{\partial x^2}, \quad (30b)$$

$$\mathbf{h}^{\text{dmg}} = -N_x (\mathbf{m} \cdot \mathbf{e}_x) \mathbf{e}_x - N_y (\mathbf{m} \cdot \mathbf{e}_y) \mathbf{e}_y - N_z (\mathbf{m} \cdot \mathbf{e}_z) \mathbf{e}_z, \quad (30c)$$

where $A = \frac{2A_{\text{exc}}}{\mu_0 M_S^2}$ includes the exchange constant of the material A_{exc} whereas the coefficients N_x , N_y , and N_z are the demagnetizing factors constrained by the normalization condition $N_x + N_y + N_z = 1$. As known, a direct computation of the demagnetizing field \mathbf{h}^{dmg} at any given point of a sample is often intractable, except in very simple cases (such as a uniformly magnetized ellipsoid or an extended system, such as a thin and elongated nanostrip). In these cases, the expression (30c) represents a commonly used and accepted approximation [42,51,53–57,59].

The expressions of \mathbf{h}^{me} and \mathbf{h}^{ani} depend on the crystal symmetry of the MS layer and are given by Eqs. (22) and (25), respectively. In particular, to properly identify the magnetoelastic field \mathbf{h}^{me} , the six independent components of the total strain tensor ϵ have to be also specified. To this aim, we preliminarily point out that, because of the small thickness of the magnetostrictive layer, it is reasonable to neglect strain variations along the z axis. Therefore, for the proposed bilayer geometry, the total strains acting on the magnetostrictive layer may be identified by applying mechanical boundary conditions at both top and bottom xy surfaces of the magnetostrictive layer. In detail, at the bottom surface, which corresponds to the interface between the thick piezoelectric actuator and the very thin magnetostrictive layer, it is realistic to assume that the three planar strains (ϵ_{xx} , ϵ_{xy} , and ϵ_{yy}) are imposed by the piezoelectric layer (via the applied electric voltage) and fully transferred to the magnetostrictive one. Consequently, these planar strains do not depend on the magnetization. In a previous work [4], the same elastic problem was studied numerically via COMSOL MULTIPHYSICS and the results suggested the possibility to neglect the in-plane shear strain ϵ_{xy} . To identify the remaining three components of the strain tensor (ϵ_{xz} , ϵ_{yz} , and ϵ_{zz}), we solve traction boundary

conditions $\sigma_{ij} n_j = t_i$ for the magnetostriction layer at its top xy surface. These conditions, with $\mathbf{n} = (0, 0, 1)$ the normal to the top surface and $\mathbf{t} = (0, 0, 0)$ the null traction acting on this surface, give rise to the three constraints

$$\sigma_{xz} = 0, \quad (31a)$$

$$\sigma_{yz} = 0, \quad (31b)$$

$$\sigma_{zz} = 0, \quad (31c)$$

which, by virtue of (3) and (18), allow to relate the strains to the magnetization:

$$\epsilon_{xz} = \lambda_E m_x m_z, \quad (32a)$$

$$\epsilon_{yz} = \lambda_E m_y m_z, \quad (32b)$$

$$\epsilon_{zz} = -\frac{c_{13}}{c_{33}} (\epsilon_{xx} + \epsilon_{yy}) + \lambda_C (1 - m_z^2) + \lambda_{33} + \frac{c_{13}}{c_{33}} [(\lambda_A + \lambda_B)(1 - m_z^2) + 2\lambda_{13}]. \quad (32c)$$

The spin-transfer torque \mathbf{t}^{stt} consists of the adiabatic and nonadiabatic contributions that are responsible for the DW distortion and motion [42,44], respectively,

$$\mathbf{t}^{\text{stt}} = -u_0 J \frac{\partial \mathbf{m}}{\partial x} - \eta u_0 J \frac{\partial \mathbf{m}}{\partial x} \wedge \mathbf{m}, \quad (33)$$

where η is the phenomenological nonadiabatic parameter and the coefficient $u_0 = g\mu_B P / (2eM_S)$ is expressed in terms of the Bohr magneton μ_B and the polarization factor of the current P .

Finally, the damping term \mathbf{t}^{d} in (28) encloses the classical Gilbert damping torque [40,45] and the nonlinear contribution arising from a rate-independent dry friction [47,48,60], namely,

$$\mathbf{t}^{\text{d}} = (\alpha_G + \gamma \alpha_D \|\dot{\mathbf{m}}\|^{-1}) (\mathbf{m} \wedge \dot{\mathbf{m}}), \quad (34)$$

where α_G and α_D are the phenomenological dimensionless parameters describing the strength of linear and nonlinear dissipation, respectively. The dry-friction dissipation is introduced to mimic the presence of crystallographic defects and disorder into the MS layer so that it could also account for pinning effects due to piezoelectric-induced strains [43,47,48,60].

By adopting spherical coordinates, the magnetization vector is given by

$$\mathbf{m} = \cos \varphi \sin \theta \mathbf{e}_x + \sin \varphi \sin \theta \mathbf{e}_y + \cos \theta \mathbf{e}_z, \quad (35)$$

being θ and φ the polar and azimuthal angles, respectively. Then, after substituting (29), (30), and (33)–(35) into the ELLG equation (28), we obtain

$$\begin{aligned} \sin \theta \dot{\varphi} - [\alpha_G + \gamma \alpha_D (\dot{\theta}^2 + \sin^2 \theta \dot{\varphi}^2)^{-1/2}] \dot{\theta} &= \gamma \left\{ -A \frac{\partial^2 \theta}{\partial x^2} + A \sin \theta \cos \theta \left(\frac{\partial \varphi}{\partial x} \right)^2 \right. \\ &\quad - \cos \theta \cos \varphi (h_x + h_x^{\text{me}} + h_x^{\text{ani}}) - \cos \theta \sin \varphi (h_y + h_y^{\text{me}} + h_y^{\text{ani}}) + \sin \theta (h_z + h_z^{\text{me}} + h_z^{\text{ani}}) \\ &\quad \left. + \sin \theta \cos \theta [N_x \cos^2 \varphi + N_y \sin^2 \varphi - N_z] \right\} - u_0 J \sin \theta \frac{\partial \varphi}{\partial x} + \eta u_0 J \frac{\partial \theta}{\partial x} \\ &\times [\alpha_G + \gamma \alpha_D (\dot{\theta}^2 + \sin^2 \theta \dot{\varphi}^2)^{-1/2}] \sin \theta \dot{\varphi} + \dot{\theta} = \gamma \left\{ A \sin \theta \frac{\partial^2 \varphi}{\partial x^2} + 2A \cos \theta \frac{\partial \theta}{\partial x} \frac{\partial \varphi}{\partial x} \right. \\ &\quad \left. + (N_x - N_y) \sin \theta \cos \varphi \sin \varphi + (h_y + h_y^{\text{me}} + h_y^{\text{ani}}) \cos \varphi - (h_x + h_x^{\text{me}} + h_x^{\text{ani}}) \sin \varphi \right\} - \eta u_0 J \sin \theta \frac{\partial \varphi}{\partial x} - u_0 J \frac{\partial \theta}{\partial x}, \quad (36) \end{aligned}$$

where the components of the magnetoelastic field (22) read as

$$h_x^{\text{me}} = \frac{2}{\mu_0 M_S^2} \sin \theta \cos \varphi (\lambda_A - \lambda_B) \left\{ \cos^2 \theta \left[(\lambda_A c_{11} + \lambda_B c_{12} - \frac{c_{13}^2}{c_{33}} (\lambda_A + \lambda_B)) \right. \right. \\ \left. \left. + \left[c_{11} \epsilon_{xx} + c_{12} \epsilon_{yy} - \frac{c_{13}^2}{c_{33}} (\epsilon_{xx} + \epsilon_{yy} - \lambda_A - \lambda_B - 2\lambda_{13}) - (\lambda_A + \lambda_{13}) c_{11} - (\lambda_B + \lambda_{13}) c_{12} \right] \right\}, \quad (37a)$$

$$h_y^{\text{me}} = \frac{2}{\mu_0 M_S^2} \sin \theta \sin \varphi (\lambda_A - \lambda_B) \left\{ \cos^2 \theta \left[(\lambda_A c_{11} + \lambda_B c_{12} - \frac{c_{13}^2}{c_{33}} (\lambda_A + \lambda_B)) \right. \right. \\ \left. \left. + \left[c_{12} \epsilon_{xx} + c_{11} \epsilon_{yy} - \frac{c_{13}^2}{c_{33}} (\epsilon_{xx} + \epsilon_{yy} - \lambda_A - \lambda_B - 2\lambda_{13}) - (\lambda_A + \lambda_{13}) c_{11} - (\lambda_B + \lambda_{13}) c_{12} \right] \right\}, \quad (37b)$$

$$h_z^{\text{me}} = \frac{2}{\mu_0 M_S^2} \cos \theta \lambda_B \left(\frac{2c_{13}^2}{c_{33}} - c_{11} - c_{12} \right) \{ \epsilon_{xx} + \epsilon_{yy} - (\lambda_A + \lambda_B + 2\lambda_{13}) + \cos^2 \theta (\lambda_A + \lambda_B) \}, \quad (37c)$$

and the anisotropy field \mathbf{h}^{ani} (25) takes the expression

$$\mathbf{h}^{\text{ani}} = \frac{2K_A}{\mu_0 M_S^2} \cos \theta \mathbf{e}_z. \quad (38)$$

By using (37c) and (38), we define the overall anisotropy field along the easy axis \mathbf{e}_z as

$$h_z^{\text{me}} + h_z^{\text{ani}} = \frac{2K_{\text{eff}}}{\mu_0 M_S^2}, \quad (39)$$

where, taking into account (32c), the effective anisotropy coefficient K_{eff} in the saturated case ($m_z = 1 \rightarrow \theta = 0$) is expressed as

$$K_{\text{eff}} = K_A + \frac{\lambda_B}{c_{13}} [(c_{11} + c_{12})c_{33} - 2c_{13}^2] (\epsilon_{zz} - \lambda_{33}). \quad (40)$$

Let us now investigate DW dynamics occurring in *steady* and *precessional* dynamical regimes [61]. As known, the *steady* regime is characterized by a rigid motion of the DW along the nanostrip axis \mathbf{e}_x with constant velocity v , fixed azimuthal angle φ_0 , and the polar angle satisfying the classical traveling wave ansatz $\theta = \theta(\xi)$, being $\xi = x - vt$ [59]. Using these assumptions, the system (36) reduces to

$$[\alpha_G v - \eta u_0 J] \theta' + \widehat{\alpha}_D = \gamma \left\{ -A \theta'' + (N_x \cos^2 \varphi_0 + N_y \sin^2 \varphi_0 - N_z) \sin \theta \cos \theta + (h_z + h_z^{\text{me}} + h_z^{\text{an}}) \sin \theta \right. \\ \left. - [(h_x + h_x^{\text{me}} + h_x^{\text{an}}) \cos \varphi_0 + (h_y + h_y^{\text{me}} + h_y^{\text{an}}) \sin \varphi_0] \cos \theta \right\}, \quad (41a)$$

$$(u_0 J - v) \theta' = \gamma \left\{ (N_x - N_y) \sin \varphi_0 \cos \varphi_0 \sin \theta + (h_y + h_y^{\text{me}} + h_y^{\text{an}}) \cos \varphi_0 - (h_x + h_x^{\text{me}} + h_x^{\text{an}}) \sin \varphi_0 \right\}, \quad (41b)$$

where the prime denotes derivative with respect to the traveling-wave variable ξ and $\widehat{\alpha}_D = \gamma \alpha_D \text{sgn}(v \theta')$. This regime takes place if the strength of the external sources is below the critical Walker breakdown value.

We recast (41b) as

$$\theta' = \Gamma (\sin \theta + k), \quad (42)$$

being

$$\Gamma = \frac{\gamma}{2(u_0 J - v)} \left[N_x - N_y + \frac{2}{\mu_0 M_S^2} (\lambda_A - \lambda_B) (c_{11} - c_{12}) (\epsilon_{yy} - \epsilon_{xx}) \right] \sin 2\varphi_0, \quad (43a)$$

$$k = \frac{2\mu_0 M_S^2 (h_y \cos \varphi_0 - h_x \sin \varphi_0)}{[\mu_0 M_S^2 (N_x - N_y) + 2(\lambda_A - \lambda_B) (c_{11} - c_{12}) (\epsilon_{yy} - \epsilon_{xx})] \sin 2\varphi_0}. \quad (43b)$$

By inserting (42) into (41a) we get

$$P \sin \theta + Q \cos \theta + R \sin \theta \cos \theta + G \sin \theta \cos^3 \theta + V = 0, \quad (44)$$

where

$$P = \Gamma (\alpha_G v - \eta u_0 J) - \gamma h_z, \quad (45a)$$

$$Q = \gamma (h_x \cos \varphi_0 + h_y \sin \varphi_0 + A \Gamma^2 k), \quad (45b)$$

$$R = \gamma \left\{ A \Gamma^2 + N_z - N_y \sin^2 \varphi_0 - N_x \cos^2 \varphi_0 + \frac{2(\psi - K_A)}{\mu_0 M_S^2} \right\}, \quad (45c)$$

$$G = \frac{2\gamma}{\mu_0 M_S^2} \left\{ (\lambda_A^2 + \lambda_B^2) c_{11} + 2\lambda_A \lambda_B c_{12} - (\lambda_A + \lambda_B)^2 \frac{c_{13}^2}{c_{33}} \right\}, \quad (45d)$$

$$V = k \Gamma (\alpha_G v - \eta u_0 J) + \widehat{\alpha}_D, \quad (45e)$$

with

$$\begin{aligned} \psi = & (\lambda_A - \lambda_B)[(c_{11} \cos^2 \varphi_0 + c_{12} \sin^2 \varphi_0)\epsilon_{xx} + (c_{12} \cos^2 \varphi_0 + c_{11} \sin^2 \varphi_0)\epsilon_{yy}] \\ & + \left[\lambda_B(c_{11} + c_{12}) - (\lambda_A + \lambda_B) \frac{c_{13}^2}{c_{33}} \right] (\epsilon_{xx} + \epsilon_{yy}) + (\lambda_A + \lambda_B + 2\lambda_{13})(\lambda_A + \lambda_B) \frac{c_{13}^2}{c_{33}} \\ & - [\lambda_A^2 + \lambda_B^2 + \lambda_{13}(\lambda_A + \lambda_B)]c_{11} - [2\lambda_A\lambda_B + \lambda_{13}(\lambda_A + \lambda_B)]c_{12}. \end{aligned} \quad (46)$$

The expression of the DW width $\delta = 1/\Gamma$ is recovered from (45) by setting $R = 0$:

$$\delta = \sqrt{\frac{A_{\text{exc}}}{K_A - \psi + \frac{\mu_0 M_S^2}{2}(N_x \cos^2 \varphi_0 + N_y \sin^2 \varphi_0 - N_z)}}. \quad (47)$$

It is interesting to notice that the traveling-wave solution (42) is formally analogous to the one found in isotropic systems when one considers the external field to be directed along an arbitrary direction [43].

For simplicity, we assume that the external magnetic field is directed along the \mathbf{e}_z axis so that $k = 0$. Under this assumption, Eq. (42) admits two steady-state solutions that represent the configurations of the two faraway domains corresponding to the classical Walker profile of a Bloch DW with θ varying between 0° and 180° . The solution of (42) thus takes the classical form

$$\theta(\xi) = 2 \arctan e^{\Gamma \xi}. \quad (48)$$

Then, performing the average of the Eq. (44) over the DW width (i.e., for $0^\circ \leq \theta \leq 180^\circ$), and taking into account that $Q = 0$ for $h_x = h_y = k = 0$, it is possible to derive the explicit expressions for the key features involved in the steady regime. The steady DW velocity is

$$v = \frac{\gamma \delta}{\alpha_G} h_z + \frac{\eta u_0}{\alpha_G} J - \frac{\pi \delta}{2\alpha_G} \widehat{\alpha}_D, \quad (49)$$

and is non-null if the values of the external sources are above the thresholds

$$J = 0 \implies h_z^{\text{TH}} = \frac{\pi}{2\gamma} \widehat{\alpha}_D, \quad (50a)$$

$$h_z = 0 \implies J^{\text{TH}} = \frac{\pi \delta}{2\eta u_0} \widehat{\alpha}_D. \quad (50b)$$

A further restriction on the DW velocity arises from (43a), which implies the existence of lower and upper Walker breakdown (WB) conditions:

$$v_1 \leq v \leq v_2, \quad (51a)$$

$$J = 0 \implies h_z^{\text{WB}} = \frac{\pi}{2\gamma} \widehat{\alpha}_D + \frac{\alpha_G}{2} \left| N_x - N_y + \frac{2}{\mu_0 M_S^2} (\lambda_A - \lambda_B)(c_{11} - c_{12})(\epsilon_{yy} - \epsilon_{xx}) \right|, \quad (51b)$$

$$h_z = 0 \implies \begin{cases} J_{\text{upper}}^{\text{WB}} = \frac{\delta}{2|\eta - \alpha_G|u_0} \left[\pi \widehat{\alpha}_D + \alpha_G \gamma \left| N_x - N_y + \frac{2}{\mu_0 M_S^2} (\lambda_A - \lambda_B)(c_{11} - c_{12})(\epsilon_{yy} - \epsilon_{xx}) \right| \right], \\ J_{\text{lower}}^{\text{WB}} = \frac{\delta}{2|\eta - \alpha_G|u_0} \left[\pi \widehat{\alpha}_D - \alpha_G \gamma \left| N_x - N_y + \frac{2}{\mu_0 M_S^2} (\lambda_A - \lambda_B)(c_{11} - c_{12})(\epsilon_{yy} - \epsilon_{xx}) \right| \right], \end{cases} \quad (51c)$$

being

$$v_1 = u_0 J - \frac{\gamma \delta}{2} \left| N_x - N_y + \frac{2}{\mu_0 M_S^2} (\lambda_A - \lambda_B)(c_{11} - c_{12})(\epsilon_{yy} - \epsilon_{xx}) \right|, \quad (52a)$$

$$v_2 = u_0 J + \frac{\gamma \delta}{2} \left| N_x - N_y + \frac{2}{\mu_0 M_S^2} (\lambda_A - \lambda_B)(c_{11} - c_{12})(\epsilon_{yy} - \epsilon_{xx}) \right|. \quad (52b)$$

When one of the breakdown conditions is violated, the DW motion occurs via a *precessional* dynamics characterized by time-dependent velocity $v(t)$ and periodic oscillations at microwave frequency with constant angular speed $\dot{\varphi} = \omega_0$. In this case, the governing system (36) reads as

$$\begin{aligned} \omega_0 \sin \theta + [\alpha_G v + \gamma \alpha_D v (v^2 \theta'^2 + \omega_0^2 \sin^2 \theta)^{-1/2} - \eta u_0 J] \theta' &= \gamma \{ [N_x \cos^2 \varphi + N_y \sin^2 \varphi - N_z] \sin \theta \cos \theta - A \theta'' \\ &\quad - [(h_x + h_x^{\text{me}} + h_x^{\text{an}}) \cos \varphi + (h_y + h_y^{\text{me}} + h_y^{\text{an}}) \sin \varphi] \cos \theta + (h_z + h_z^{\text{me}} + h_z^{\text{an}}) \sin \theta \}, \\ [\alpha_G + \gamma \alpha_D (v^2 \theta'^2 + \omega_0^2 \sin^2 \theta)^{-1/2}] \sin \theta \omega_0 + (u_0 J - v) \theta' & \\ = \gamma \{ (N_x - N_y) \sin \theta \cos \varphi \sin \varphi + (h_y + h_y^{\text{me}} + h_y^{\text{an}}) \cos \varphi - (h_x + h_x^{\text{me}} + h_x^{\text{an}}) \sin \varphi \}. & \end{aligned} \quad (53)$$

Under the assumption that the traveling-wave profile given by (42) is unchanged, Eq. (53) can be rewritten in the form

$$\omega_0 + \Gamma[\alpha_G + \gamma\alpha_D(v^2\Gamma^2 + \omega_0^2)^{-1/2}]v = \gamma h_z + \Gamma\eta u_0 J, \quad (54a)$$

$$[\alpha_G + \gamma\alpha_D(v^2\Gamma^2 + \omega_0^2)^{-1/2}]\omega_0 = \Gamma(v - u_0 J) + \gamma \sin\varphi_0 \cos\varphi_0 \left\{ N_x - N_y + \frac{2}{\mu_0 M_S^2}(\lambda_A - \lambda_B)(c_{11} - c_{12})(\epsilon_{yy} - \epsilon_{xx}) \right\}, \quad (54b)$$

where all the quantities have been evaluated at the center of the DW ($\theta = \frac{\pi}{2}$). Then, by performing the average of the equations (54) over a period of precession, under the restriction $\Gamma\bar{v} \ll \omega_0$, we deduce the system of equations

$$\omega_0 + \alpha_G \Gamma \bar{v} = \gamma h_z + \Gamma \eta u_0 J, \quad (55a)$$

$$\alpha_G \omega_0 + \gamma \alpha_D = \Gamma(\bar{v} - u_0 J), \quad (55b)$$

and allows to express the precessional DW velocity for hexagonal crystals as

$$\bar{v} = \frac{\alpha_G \gamma \delta}{1 + \alpha_G^2} h_z + \frac{(1 + \alpha_G \eta) u_0}{1 + \alpha_G^2} J + \frac{\gamma \delta}{1 + \alpha_G^2} \alpha_D. \quad (56)$$

As it can be observed, magnetoelastic effects do not formally alter the structure of the classical solution obtained in isotropic systems [43]. However, piezoinduced strains may now affect the DW mobility under an applied magnetic field (not under an electric current) as well as the upward shift of the average DW velocity through the DW width δ only.

Identification of the magnetostrictive coefficients

In this section, we present a possible strategy to obtain an indirect measurement of all the *six* components of the fourth-order magnetostriction tensor of transversely isotropic hexagonal crystals. Since four of the six coefficients are known in the literature ($\lambda_A, \lambda_B, \lambda_C, \lambda_E$), two extra independent conditions are required for the identification of the remaining two ($\lambda_{13}, \lambda_{33}$). To achieve this goal, in Sec. III we inspected the functional dependence of the key dynamical features involved in the strain-mediated DW motion on magnetostriction.

Results of the investigations carried out in Sec. III showed that two quantities satisfy the above requirement: the effective anisotropy coefficient K_{eff} and the DW width δ (or a quantity directly related to it, such as the DW velocity v or the DW mobility induced by the applied field $\partial v / \partial h$ or the electric current $\partial v / \partial J$). Indeed, the inspection of their magnetostriction dependence reveals that $K_{\text{eff}} = K_{\text{eff}}(\lambda_B, \lambda_{33})$ while $\delta = \delta(\lambda_A, \lambda_B, \lambda_{13})$. Moreover, since Eqs. (40) and (47) are independent from the four conditions (19a)–(19d), they provide a possible means to solve the present identification issue. It is interesting to notice that these two quantities are quite easily accessible via both experiments and numerical simulations, which makes the proposed strategy feasible. The identification procedure can be further simplified by evaluating these quantities in the absence of applied strains, with the advantage of reducing measurement errors. In the unstrained case, K_{eff} reduces to

$$K_{\text{eff}_0} \equiv K_{\text{eff}}|_{\epsilon=0} = K_A - \frac{\lambda_B}{c_{13}} [(c_{11} + c_{12})c_{33} - 2c_{13}^2] \lambda_{33}, \quad (57)$$

and δ reduces to

$$\begin{aligned} \delta_0 &\equiv \delta|_{\epsilon=0} \\ &= \sqrt{\frac{A_{\text{exc}}}{K_A - \psi_0 + \frac{\mu_0 M_S^2}{2}(N_x \cos^2 \varphi_0 + N_y \sin^2 \varphi_0 - N_z)}}, \end{aligned} \quad (58)$$

where ψ_0 is the value of the parameter ψ of Eq. (46) in the unstrained case:

$$\begin{aligned} \psi_0 &\equiv \psi|_{\epsilon=0} = (\lambda_A + \lambda_B + 2\lambda_{13})(\lambda_A + \lambda_B) \frac{c_{13}^2}{c_{33}} \\ &\quad - [\lambda_A^2 + \lambda_B^2 + \lambda_{13}(\lambda_A + \lambda_B)] c_{11} \\ &\quad - [2\lambda_A \lambda_B + \lambda_{13}(\lambda_A + \lambda_B)] c_{12}. \end{aligned} \quad (59)$$

Since the material parameters, the elastic constants, and the magnetostriction constants $\lambda_A, \lambda_B, \lambda_C$, and λ_E are known, the extra conditions (57) and (58) allow to determine the unknowns λ_{13} and λ_{33} and, consequently, all the Z_{ijkl} components of the magnetostriction tensor \mathbb{Z} of a transversely isotropic hexagonal crystal via Eqs. (19).

IV. NUMERICAL RESULTS

In Sec. II, we pointed out that, in order to describe magnetoelastic effects in hexagonal crystals, the knowledge of all six components of the magnetostriction tensor \mathbb{Z} is required. Since the number of independent measurements of differential scalar strain is limited to four, in Sec. III A we presented a possible strategy to identify all the magnetostrictive coefficients Z_{ijkl} by considering the two extra constraints arising from Eqs. (57) and (58). To provide a numerical illustrative solution of this issue, we refer to the interesting work by Shepley *et al.* [6], who provided the values of the effective anisotropy coefficient K_{eff} and DW velocity in a hexagonal cobalt-based alloy (Pt/Co/Pt) in the presence and in the absence of voltage-induced strains (see, in particular, Fig. 1 of that paper). We use parameters extracted from the literature for CoPt alloys and Co-based materials, which are reported in Table I.

We preliminarily verify that the above setup is consistent with experimental data. To this aim, we estimate the variation of the effective anisotropy constant with the out-of-plane component of the strain tensor. According to our expression (40), this quantity is given by

$$\frac{\partial K_{\text{eff}}}{\partial \epsilon_{zz}} = \frac{\lambda_B}{c_{13}} [(c_{11} + c_{12})c_{33} - 2c_{13}^2] = -9.98 \times 10^6 \text{ J/m}^3. \quad (60)$$

The resulting decreasing linear dependence confirms the trend shown in Fig. 1(b) of Ref. [6] and the obtained value is also in close agreement with the approximated one provided by

TABLE I. Material parameters used for the hexagonal Co-based magnetostrictive materials.

Quantity	Unit	Value	Ref.
λ_A		-45×10^{-6}	[31,32]
λ_B		-95×10^{-6}	[31,32]
λ_C		$+110 \times 10^{-6}$	[31,32]
λ_E		-232×10^{-6}	[31,32]
K_A	J/m ³	2×10^5	[6]
$\mu_0 M_S$	T	1.63	[6]
A_{exc}	pJ/m	14	[62]
α_G		0.01	[63]
c_{11}	GPa	320	[64]
c_{12}	GPa	190	[64]
c_{13}	GPa	265	[64]
c_{33}	GPa	330	[64]
c_{44}	GPa	75	[34,38]
N_x		0.6417	Assumed
N_y		0.0093	Assumed
N_z		0.3490	Assumed
φ_0	deg	10	Assumed

the same authors and given by $\frac{3}{2}Y\lambda_S = -9.45 \times 10^6$ J/m³, with $Y = 180$ GPa being the average of the Young's moduli of bulk Co and Pt and $\lambda_S = -3.5 \times 10^{-5}$ the saturation magnetostriction [see Eq. (4) of Ref. [6]]. Therefore, by solving numerically the system (57) and (58) with $K_{\text{eff}0} = 210$ kJ/m³ and $\delta_0 = 5.3$ nm, we obtain $\lambda_{13} = -580 \times 10^{-6}$ and $\lambda_{33} = 1.002 \times 10^{-3}$ and, using (19), we can deduce *all* the values of the components of the fourth-order magnetostriction tensor \mathbb{Z} :

$$Z_{1111} = -625 \times 10^{-6}, \quad (61a)$$

$$Z_{1122} = -675 \times 10^{-6}, \quad (61b)$$

$$Z_{1133} = -580 \times 10^{-6}, \quad (61c)$$

$$Z_{3311} = +1.112 \times 10^{-3}, \quad (61d)$$

$$Z_{3333} = +1.002 \times 10^{-3}, \quad (61e)$$

$$Z_{2323} = -116 \times 10^{-6}. \quad (61f)$$

Finally, by using the above parameters, in Fig. 2 we represent the behavior of DW width δ [Eq. (47)], effective

anisotropy coefficient K_{eff} [Eq. (40)], and field-driven steady DW velocity v [Eq. (49)] as a function of the out-of-plane piezoeinduced strain ϵ_{zz} . In addressing the comparison with experimental data, we consider the out-of-plane strain in the same range as in Ref. [6], namely, $\epsilon_{zz} \in [-4 \times 10^{-4}, +10 \times 10^{-4}]$. Moreover, we hypothesize that the dry-friction coefficient α_D may depend or not on the out-of-plane strain, i.e., $\alpha_D = 10^{-3}(1 - \nu\epsilon_{zz})$, with $\nu = 500$ or 0, respectively. As it can be argued, the increase of strain yields a reduction of K_{eff} [see Fig. 2(b)] and an increase of both δ [Fig. 2(a)] and v [Fig. 2(c)], consistently with experimental results [6]. Notice that the upward shift of DW velocity with strain holds independently of the possible dependence of α_D on ϵ_{zz} .

V. CONCLUSIONS

In this work, we analytically investigated magnetostrictive effects arising in transversely isotropic hexagonal crystals. We focused our attention on a critical issue concerning the identification of the *six* independent components of the fourth-order magnetostriction tensor. Indeed, despite this tensor constitutes the primitive object from which all related quantities of interest in micromagnetism are computed, its role has been somehow overlooked in the recent literature. In particular, the only available information on such a tensor dated back to Mason's work [23] where the explicit expression of the differential scalar strain in an arbitrary direction was provided in terms of just *four* conditions relating the magnetostrictive coefficients. Therefore, the identification of the magnetostriction tensor for a hexagonal crystal required two additional constraints, independent from the previous ones, to be deduced.

In this work, we solved this issue by inspecting the functional dependence of the most relevant physical quantities involved in the motion of a DW along the major axis of a thin magnetostrictive nanostrip placed on the top of a thick piezoelectric actuator. We found that the knowledge of the effective anisotropy coefficient and the DW width allows to determine *all* the six magnetostrictive coefficients and, consequently, to fully characterize the magnetoelastic field. As a further advantage of our identification procedure, the two above quantities can be even measured in the absence of applied strains. By using the acquired complete setup

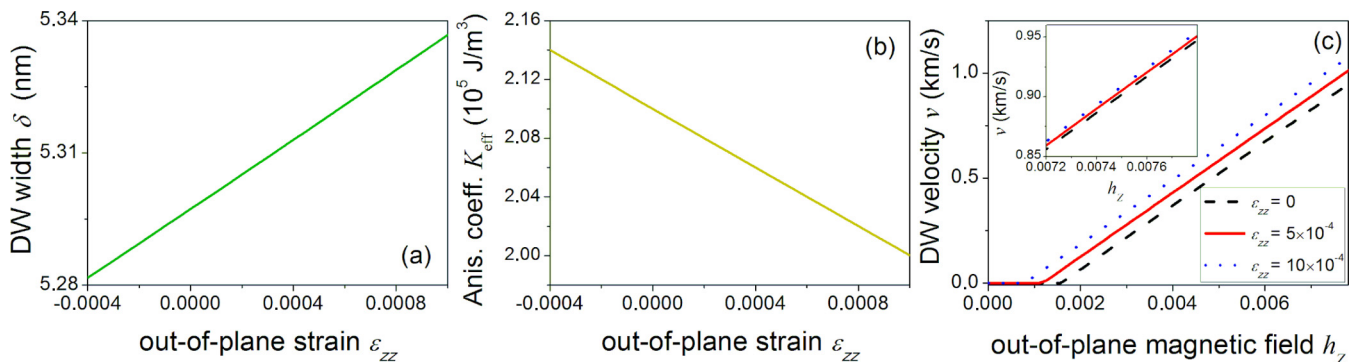


FIG. 2. Strain dependence of (a) DW width δ , (b) effective anisotropy coefficient K_{eff} , and (c) field-driven steady DW velocity v . In the main panel (inset) of (c), it is assumed that the dry-friction coefficient α_D depends linearly (does not depend) on strain.

of parameters, a quantitative agreement with some recent experimental observations on strain-mediated domain wall motion in a cobalt-based alloy (Pt/Co/Pt) has been also achieved.

We believe that the results presented in this work might be useful for both theoreticians and experimentalists. Our findings might be exploited by the former to properly account for the magnetostriction dependence of the physical quantities characterizing a transversely isotropic crystal, and by the latter to design more performing multiferroic devices.

ACKNOWLEDGMENTS

This work has been supported by INdAM-GNFM (Italian Institute of High Mathematics and Italian Group of Mathematical Physics) (G.C., G.V.), MIUR (Italian Ministry of Education, University and Research) through Project PRIN2017 No. 2017YBKNCE, “Multiscale phenomena in Continuum Mechanics: singular limits, off-equilibrium and transitions” (G.C., G.V.), and NSERC (Natural Sciences and Engineering Research Council of Canada) through the NSERC Discovery Grant No. RGPIN-2015-06027 [S.F.].

-
- [1] W. Eerenstein, N. D. Mathur, and J. F. Scott, Multiferroic and magnetoelectric materials, *Nature (London)* **442**, 759 (2006).
- [2] C. A. F. Vaz, J. Hoffman, C. H. Ahn, and R. Ramesh, Magnetoelastic coupling effects in multiferroic complex oxide composite structures, *Adv. Mater.* **22**, 2900 (2010).
- [3] M. Balinskiy, A. C. Chavez, A. Barra, H. Chiang, G. P. Carman, and A. Khitun, Magnetoelastic spin wave modulator based on synthetic multiferroic structure, *Sci. Rep.* **8**, 10867 (2018).
- [4] N. Lei, T. Devolder, G. Agnus, P. Aubert, L. Daniel, J.-V. Kim, W. Zhao, T. Trypiniotis, R. P. Cowburn, C. Chappert *et al.*, Strain-controlled magnetic domain wall propagation in hybrid piezoelectric/ferromagnetic structures, *Nat. Commun.* **4**, 1378 (2013).
- [5] E. De Ranieri, P. E. Roy, D. Fang, E. K. Vehstedt, A. C. Irvine, D. Heiss, A. Casiraghi, R. P. Champion, B. L. Gallagher, T. Jungwirth, and J. Wunderlich, Piezoelectric control of the mobility of a domain wall driven by adiabatic and non-adiabatic torques, *Nat. Mater.* **12**, 808 (2013).
- [6] P. M. Shepley, A. W. Rushforth, M. Wang, G. Burnell, and T. A. Moore, Modification of perpendicular magnetic anisotropy and domain wall velocity in Pt/Co/Pt by voltage-induced strain, *Sci. Rep.* **5**, 7921 (2015).
- [7] J. M. Hu, T. Yang, K. Momeni, X. Cheng, L. Chen, S. Lei, S. Zhang, S. Trolrier-McKinstry, V. Gopalan, G. P. Carman *et al.*, Fast magnetic domain-wall motion in a ring-shaped nanowire driven by a voltage, *Nano Lett.* **16**, 2341 (2016).
- [8] D. A. Filippov, G. S. Radchenko, T. O. Firsova, and T. A. Galkina, A theory of the inverse magnetoelectric effect in layered magnetostrictive–piezoelectric structures, *Phys. Solid State* **59**, 878 (2017).
- [9] P. Zhou, A. V. Singh, Z. Li, M. A. Popov, Y. Liu, D. A. Filippov, T. Zhang, W. Zhang, P. J. Shah, B. M. Howe *et al.*, Magnetoelastic Interactions in Composites of Ferrite Films on Lattice-Matched Substrates and Ferroelectrics, *Phys. Rev. Appl.* **11**, 054045 (2019).
- [10] A. Hubert and R. Schäfer, *Magnetic Domains: The Analysis of Magnetic Microstructures* (Springer, Berlin, 2008).
- [11] S. Chikazumi and C. D. Graham, *Physics of Ferromagnetism* (Oxford University Press, Oxford, 2009).
- [12] B. D. Cullity and C. D. Graham, *Introduction to Magnetic Materials* (Wiley, Hoboken, NJ, 2009).
- [13] K. Richter, R. Varga, and A. Zhukov, Influence of the magnetoelastic anisotropy on the domain wall dynamics in bistable amorphous wires, *J. Phys.: Condens. Matter* **24**, 296003 (2012).
- [14] T. Mathurin, S. Giordano, Y. Dusch, N. Tiercelin, P. Pernod, and V. Preobrazhensky, Mechanically driven domain wall movement in magnetoelastic nanomagnets, *Eur. Phys. J. B* **89**, 169 (2016).
- [15] K. E. Kim, and C. H. Yang, Local magnetostriction measurement in a cobalt thin film using scanning probe microscopy, *AIP Adv.* **8**, 105125 (2018).
- [16] Y. C. Shu, M. P. Lin, and K. C. Wu, Micromagnetic modeling of magnetostrictive materials under intrinsic stress, *Mech. Mater.* **36**, 975 (2004).
- [17] L. Daniel, O. Hubert, N. Buiron, and R. Billardon, Reversible magneto-elastic behavior: A multiscale approach, *J. Mech. Phys. Solids* **56**, 1018 (2008).
- [18] J. M. Hu, G. Sheng, J. X. Zhang, C. W. Nan, and L. Q. Chen, Phase-field simulation of strain-induced domain switching in magnetic thin films, *Appl. Phys. Lett.* **98**, 112505 (2011).
- [19] J. Wang and J. Zhang, A real-space phase field model for the domain evolution of ferromagnetic materials, *Int. J. Solids Struct.* **50**, 3597 (2013).
- [20] F. S. Mballa-Mballa, O. Hubert, S. He, S. Depeyre, and P. Meiland, Micromagnetic modeling of magneto-mechanical behavior, *IEEE Trans. Magn.* **50**, 1 (2014).
- [21] C. Y. Liang, S. M. Keller, A. E. Sepulveda, A. Bur, W. Y. Sun, K. Wetzlar, and G. P. Carman, Modeling of magnetoelastic nanostructures with a fully coupled mechanical-micromagnetic model, *Nanotechnology* **25**, 435701 (2014).
- [22] T. A. Ostler, R. Cuadrado, R. W. Chantrell, A. W. Rushforth, and S. A. Cavill, Strain Induced Vortex Core Switching in Planar Magnetostrictive Nanostructures, *Phys. Rev. Lett.* **115**, 067202 (2015).
- [23] W. P. Mason, Derivation of magnetostriction and anisotropic energies for hexagonal, tetragonal, and orthorhombic crystals, *Phys. Rev.* **96**, 302 (1954).
- [24] L. Bañas, A numerical method for the Landau–Lifshitz equation with magnetostriction, *Math. Meth. Appl. Sci.* **28**, 1939 (2005).
- [25] J. E. Marsden and T. J. R. Hughes, *Mathematical Foundations of Elasticity* (Prentice-Hall, Englewood Cliffs, NJ, 1983).
- [26] R. W. Ogden, *Non-linear Elastic Deformations* (Dover, New York, 1997).
- [27] S. Federico, A. Grillo, and S. Imatani, The linear elasticity tensor of incompressible materials, *Math. Mech. Solids* **20**, 643 (2015).
- [28] J. X. Zhang and L. Q. Chen, Phase-field microelasticity theory and micromagnetic simulations of domain structures in giant magnetostrictive materials, *Acta Mater.* **53**, 2845 (2005).
- [29] L. J. Walpole, Fourth-rank tensors of the thirty-two crystal classes: Multiplication tables, *Proc. R. Soc. London A* **391**, 149 (1984).
- [30] S. Federico, G. Consolo, and G. Valenti, Tensor representation of magnetostriction for all crystal classes, *Math. Mech. Solids* **24**, 2814 (2019).

- [31] R. M. Bozorth, Magnetostriction and crystal anisotropy of single crystals of hexagonal cobalt, *Phys. Rev.* **96**, 311 (1954).
- [32] A. Hubert, W. Unger, and J. Kranz, Measurement of the magnetostriction constants of cobalt as a function of temperature, *Z. Phys.* **224**, 148 (1969).
- [33] E. Callen and H. B. Callen, Magnetostriction, forced magnetostriction, and anomalous thermal expansion in ferromagnets, *Phys. Rev.* **139**, A455 (1965).
- [34] P. Bruno, Magnetic surface anisotropy of cobalt and surface roughness effects within Neel's model, *J. Phys. F: Met. Phys.* **18**, 1291 (1988).
- [35] D. Sander, The correlation between mechanical stress and magnetic anisotropy in ultrathin films, *Rep. Prog. Phys.* **62**, 809 (1999).
- [36] T. Gutjahr-Löser, D. Sander, and J. Kirschner, Magnetoelastic coupling in Co thin films on W(0 0 1), *J. Magn. Magn. Mater.* **220**, 1 (2000).
- [37] R. Koch, C. Pampuch, H. Yamaguchi, A. K. Das, A. Ney, L. Däweritz, and K. H. Ploog, Magnetoelastic coupling of MnAs/GaAs (001) close to the phase transition, *Phys. Rev. B* **70**, 092406 (2004).
- [38] V. Z. C. Paes and D. H. Mosca, Field-induced lattice deformation contribution to the magnetic anisotropy, *J. Appl. Phys.* **112**, 103920 (2012).
- [39] L. D. Landau and E. M. Lifshitz, On the theory of the dispersion of magnetic permeability in ferromagnetic bodies, *Phys. Z. Sowjetunion* **8**, 153 (1935).
- [40] T. L. Gilbert, A phenomenological theory of damping in ferromagnetic materials, *IEEE Trans. Magn.* **40**, 3443 (2004).
- [41] L. Berger, Emission of spin waves by a magnetic multilayer traversed by a current, *Phys. Rev. B* **54**, 9353 (1996).
- [42] S. Zhang and Z. Li, Roles of Nonequilibrium Conduction Electrons on the Magnetization Dynamics of Ferromagnets, *Phys. Rev. Lett.* **93**, 127204 (2004).
- [43] G. Consolo and G. Valenti, Analytical solution of the strain-controlled magnetic domain wall motion in bilayer piezoelectric/magnetostrictive nanostructures, *J. Appl. Phys.* **121**, 043903 (2017).
- [44] A. Thiaville, Y. Nakatani, J. Miltat, and Y. Suzuki, Micromagnetic understanding of current-driven domain wall motion in patterned nanowires, *Europhys. Lett.* **69**, 990 (2005).
- [45] V. Tiberkevich and A. Slavin, Nonlinear phenomenological model of magnetic dissipation for large precession angles: Generalization of the gilbert model, *Phys. Rev. B* **75**, 014440 (2007).
- [46] G. Consolo, B. Azzaroni, L. Lopez-Diaz, G. Gerhart, E. Bankowski, V. Tiberkevich, and A. N. Slavin, Micromagnetic study of the above-threshold generation regime in a spin-torque oscillator based on a magnetic nanocontact magnetized at an arbitrary angle, *Phys. Rev. B* **78**, 014420 (2008).
- [47] G. Consolo, C. Curró, E. Martinez, and G. Valenti, Mathematical modeling and numerical simulation of domain wall motion in magnetic nanostrips with crystallographic defects, *Appl. Math. Model.* **36**, 4876 (2012).
- [48] G. Consolo and G. Valenti, Traveling wave solutions of the one-dimensional extended Landau-Lifshitz-Gilbert equation with nonlinear dry and viscous dissipations, *Acta Appl. Math.* **122**, 141 (2012).
- [49] G. Consolo, C. Curró, and G. Valenti, Curved domain walls dynamics driven by magnetic field and electric current in hard ferromagnets, *Appl. Math. Model.* **38**, 1001 (2014).
- [50] L. Thomas, M. Hayashi, X. Jiang, R. Moriya, C. Rettner, and S. S. P. Parkin, Oscillatory dependence of current-driven magnetic domain wall motion on current pulse length, *Nature (London)* **443**, 197 (2006).
- [51] A. Mougín, M. Cormier, J. P. Adam, P. J. Metaxas, and J. Ferre, Domain wall mobility, stability and Walker breakdown in magnetic nanowires, *Europhys. Lett.* **78**, 57007 (2007).
- [52] S. W. Jung, W. Kim, T. D. Lee, K. J. Lee, and H. W. Lee, Current-induced domain wall motion in a nanowire with perpendicular magnetic anisotropy, *Appl. Phys. Lett.* **92**, 202508 (2008).
- [53] G. Malinowski, O. Boulle, and M. Klauí, Current-induced domain wall motion in nanoscale ferromagnetic elements, *J. Phys. D: Appl. Phys.* **44**, 384005 (2011).
- [54] O. Bou Matar, J. F. Robillard, J. O. Vasseur, A. C. Hladky-Hennion, P. A. Deymier, P. Pernod, and V. Preobrazhensky, Band gap tunability of magneto-elastic phononic crystal, *J. Appl. Phys.* **111**, 054901 (2012).
- [55] A. Goussev, R. G. Lund, J. M. Robbins, V. Slustikov, and C. Sonnenberg, Domain wall motion in magnetic nanowires: an asymptotic approach, *Proc. R. Soc. London A* **469**, 20130308 (2013).
- [56] W. Wang, M. Dvornik, M.-A. Bisotti, D. Chernyshenko, M. Beg, M. Albert, A. Vansteenkiste, B. V. Waeyenberge, A. N. Kuchko, V. V. Kruglyak, and H. Fangohr, Phenomenological description of the nonlocal magnetization relaxation in magnonics, spintronics, and domain-wall dynamics, *Phys. Rev. B* **92**, 054430 (2015).
- [57] A. Skaugen, P. Murray, and L. Laurson, Analytical computation of the demagnetizing energy of thin-film domain walls, *Phys. Rev. B* **100**, 094440 (2019).
- [58] G. Consolo, L. Lopez-Diaz, B. Azzaroni, I. Krivorotov, V. Tiberkevich, and A. Slavin, Excitation of spin waves by a current-driven magnetic nanocontact in a perpendicularly magnetized waveguide, *Phys. Rev. B* **88**, 014417 (2013).
- [59] N. L. Schryer and L. R. Walker, The motion of 180° domain walls in uniform dc magnetic fields, *J. Appl. Phys.* **45**, 5406 (1974).
- [60] W. Baltensperger and J. S. Helman, A model that gives rise to effective dry friction in micromagnetics, *J. Appl. Phys.* **73**, 6516 (1993).
- [61] P. J. Metaxas, J. P. Jamet, A. Mougín, M. Cormier, J. Ferré, V. Baltz, B. Rodmacq, B. Dieny, and R. L. Stamps, Creep and Flow Regimes of Magnetic Domain-Wall Motion in Ultrathin Pt/Co/Pt Films with Perpendicular Anisotropy, *Phys. Rev. Lett.* **99**, 217208 (2007).
- [62] C. Eyrieh, W. Huttema, M. Arora, E. Montoya, F. Rashidi, C. Burrowes, B. Kardasz, E. Girt, B. Heinrich, O. N. Mryasov *et al.*, Exchange stiffness in thin film Co alloys, *J. Appl. Phys.* **111**, 07C919 (2012).
- [63] M. Oogane, T. Wakitani, S. Yakata, R. Yilgin, Y. Ando, A. Sakuma, and T. Miyazaki, Magnetic damping in ferromagnetic thin films, *Jpn. J. Appl. Phys.* **45**, 3889 (2006).
- [64] N. Nakamura, H. Ogi, M. Hirao, and T. Ono, Elastic constants and magnetic anisotropy of Co/Pt superlattice thin films, *Appl. Phys. Lett.* **86**, 111918 (2005).